

GPS Modernization: Capabilities of the New Civil Signals

Invited Paper for the Australian International Aerospace Congress
Brisbane, 29 July – 1 August 2003

by Professor Per Enge, Stanford University

Biography: Per Enge is a Professor of Aeronautics and Astronautics at Stanford University. He is also Associate Chair of the Department, and Director of the GPS Research Laboratory. He works on the integrity machines that provide real time error bounds for the Global Positioning System (GPS). He also works on techniques to harden our navigation systems to radio frequency interference. Per has received the Kepler, Thurlow and Burka Awards from the Institute of Navigation for his work.

Abstract: Currently, the Global Positioning System (GPS) is undergoing stunning changes that will enhance both military and civil capabilities. We say that GPS is being modernized. In fact, this modernization is a fabric of change that includes three elements. It includes integrity machines, which are monitors that provide error bounds to safety-critical users in real time. It also includes a family of techniques to protect GPS users from accidental and malevolent radio frequency interference (RFI). Most of these RFI hardening techniques are based on so-called navigation signals of opportunity, such as inertial measurements or terrestrial radio navigation. Finally, GPS modernization includes new satellite signals that will provide the benefits of frequency diversity. Over the next ten years, a second civil signal, at 1227.60 MHz, and a third civil signal, at 1176.45 MHz, will join the current civil signal at 1575.42 MHz. These new signals will improve the fundamental signal acquisition and tracking performance of the GPS receiving engine. They will also enable a new family of alternatives for mitigating the ionospheric errors that currently limit the accuracy of GPS. This paper will focus on the new civil signals and the capabilities they enable.

1 Introduction

The Global Positioning System (GPS) was developed by the U.S. Department of Defense (DoD) to provide precise estimates of position, velocity, and time to users worldwide. The DoD approved the basic architecture of the system in 1973, the first satellite was launched in 1978, and the system was declared operational in 1995. Today, GPS serves over twenty million users with a breath-taking variety of applications built on these basic capabilities.

Even though civilian use was anticipated from the beginning, the system was primarily designed to serve a predicted total of 40,000 military users. Civil applications began with a trickle of survey applications, and grew to the current torrent that includes timing, land transportation, civil aviation, maritime commerce, surveying and mapping, construction, mining, agriculture, earth sciences, electric power systems, telecommunications, and outdoor recreational activities. Today, the GPS industry ships over *100,000 receivers per month* to civilian users.

A GPS user can typically estimate location with an accuracy of better than 10 meters, and time to better than 100 nanoseconds. We call this the stand-alone or unaugmented capability of

GPS, because it does not require the user to install any local infrastructure – he or she simply roves the countryside with an off-the-shelf GPS receiver.

If better accuracy is required, then differential GPS (DGPS) may be used. DGPS does require local infrastructure, including a reference receiver at a known location and a data link from the reference receiver to the roving user. The reference receiver compares the GPS measurements to those that should exist at the known location. The difference is broadcast from the reference to the rover and used to correct the measurements made by the rover. If the reference-to-rover separation is less than 10 kilometers, than the rover can achieve centimeter accuracy. At 100 kilometers, accuracies of 1 meter can be achieved. Please refer to P. Misra and P. Enge, 2001 for full error analyses of stand alone GPS and differential GPS.

Importantly, GPS is not the only global navigation satellite system. The Russians maintain a similar system called GLONASS, and the Europeans are just now embarking on the development of a system called Galileo. We limit our discussion to GPS, but the interested reader is referred to Daly and Misra, 1996 for more on GLONASS and Galileo's World for more on the European System.

Currently, GPS is undergoing substantive changes that will enhance both military and civil capabilities. We say that GPS is being modernized. In fact, modernization is a fabric of change with the following elements.

- *Integrity machines* provide error bounds to safety-critical users in real time. The first of these, the Wide Area Augmentation System or WAAS, began operation on July 10, 2003. These systems are briefly described in Section 2.
- *Navigation signals of opportunity* refer to all the other signals (inertial and radio) that will be used to harden GPS users against accidental and malevolent radio frequency interference (RFI). They will also be used to extend location services indoors and downtown. This important component of modernization is briefly described in Section 3.
- *Frequency diversity* refers to the new GPS signals that will be radiated at L2=1227.60 MHz and L5=1176.45 MHz. These new signals will join the current signal at L1=1575.42 MHz, and are described in Section 4. They will significantly improve signal tracking and acquisition, and these improvements are described in Section 5. As described in Section 6, the new signals will also enable a new level of accuracy.

Section 7 is a brief summary.

2 Integrity Machines: Real Time Error Bounds

To enable a host of safety benefits, civil aviation organizations worldwide are deploying GPS augmentation systems that improve and measure the performance of GPS in real time. One of these is a *local area* augmentation system (LAAS) and each LAAS serves one airport. The other is a *wide area* augmentation system (WAAS) that serves continental areas. The International Civil Aviation Organization (ICAO) has standards for both of these architectures. The ICAO documents refer to the LAAS as a ground based augmentation system (GBAS), and they refer to the WAAS as a space based augmentation system (SBAS) for reasons that will soon be apparent.

Both WAAS and LAAS are differential GPS systems. They measure GPS performance with GPS receivers at known reference locations. These reference receivers compare their GPS measurements to those that should exist at their known locations. The differences are converted to *corrections* and *error bounds* that are broadcast to participating aircraft in real-time. The

corrections are applied by the avionics and improve the accuracy of GPS from ten meters to one meter or better.

LAAS is a *local area* differential GPS system, because all reference receivers are placed on the property of the airport to be served. LAAS corrections are nearly perfect for aircraft approaching the subject airport. The LAAS corrections and error bounds are broadcast to the approaching aircraft using a line-of-sight VHF transmitter that is also located on the airport property. The broadcast system is referred to as a VHF data link or VDL. ICAO refers to these systems as ground-based augmentation systems (GBAS), because the data link is a terrestrial radio.

WAAS is a *wide area* differential GPS system. In contrast to LAAS, WAAS reference stations span continental areas, and WAAS develops a four dimensional correction for each satellite. One element of this 4-tuple corrects the satellite clock and the remaining three correct the satellite ephemeris (location). WAAS also sends a grid of ionospheric errors for the region spanned by the SBAS ground system. These corrections are valid across the area spanned by the reference stations, and so they are broadcast to users through a geostationary satellite with a large coverage footprint. Since satellites are used for the data link, ICAO refers to such systems as space-based augmentation systems (SBAS). The geostationary satellite modulates the WAAS data onto a signal that is in the GPS L1 band and resembles the GPS signal, and this signal is synchronized to GPS time. Consequently, the geostationary satellite serves two purposes: it is a data link and it can augment the normal suite of GPS ranging measurements.

Even though LAAS and WAAS develop corrections to improve accuracy, their truly essential purpose is to broadcast real-time error-bounds. These bounds are called protection levels (PLs) and must over bound the true position error under all conditions and in real time. The pilot uses the current PL to determine whether a particular operation is safe. If the protection level is smaller than the alarm limit (AL) required for a particular operation, then the pilot may fly that procedure. If the PL fails to bound the error, then the pilot may attempt a landing that is not safe and integrity has failed. On the other hand, the PLs cannot be too conservative - otherwise the full capability of the system will not be utilized.

The essential purpose of LAAS and WAAS is to provide real time error bounds or protection levels (*PL*) that meet the following requirement.

$$\Pr(\varepsilon > PL) < 10^{-7}$$

$$PL(z) = \min \left\{ q \left| \sum_i \Pr(\varepsilon > q | H_i \cap z) \Pr(H_i | z) < 10^{-7} \right. \right\} \quad (1)$$

According to the top equation, the protection level (*PL*) must overbound the true error experience by the user () with a probability of $1-10^{-7}$. The second equation develops this basic requirement. As shown, the protection level is based on the measurements that are currently available from the reference receivers (*z*). This data is used to ascertain the probability that certain specified hazards may be in force. Example hazards include an active ionosphere, satellite signal failures, signal reflections near the receiving antennas, and radio frequency interference. $\Pr(H_i | z)$ is the probability that hazard *i* is true given the current data. The PL should be the minimum value that almost certainly overbounds the true error given that the system must operate in the presence of the specified list of potential hazards, $\{H_i\}_{i=1}^l$.

Importantly, LAAS and WAAS are structured so that individual countries retain control over the safety of navigation within their borders. Indeed, each government has responsibility for safe navigation within its borders, and today they rely on in-country, terrestrial equipment to execute this sovereign responsibility. With LAAS and WAAS, they still have a national mechanism to monitor and override the signals that come from a shared international satellite navigation system. This mechanism is under sovereign control, but conforms to international standards, so that an aircraft need not carry multiple sets of avionics simply because it crosses political boundaries. WAAS became operational in the United States on July 10, 2003. The Europeans and Japanese will deploy similar systems within a few years. Ground-based augmentation systems will come on-line in a similar time frame.

3 Using Signals of Opportunity to Harden GPS

GPS signals travel 20,000 kilometers from medium-earth orbit to the surface of the Earth, and so the received signals are extremely weak. Consequently, they are vulnerable to radio frequency interference (RFI) and signal obstructions. The performance of the receiver depends on the received carrier power to noise density ratio, which is nominally given by

$$\frac{C}{N_0} = \frac{G_R P_S}{N_0} = \frac{G_R P_S}{kT_A + kT_0 (F_{LNA} L_{\text{cable/filter}})} \quad (2)$$

The received power in the nominal GPS signal is P_S Watts, and is approximately equal to 10^{-16} Watts or -160 dBW or -130 dBm, where

$$\begin{aligned} x_{\text{dBW}} &= 10 \log_{10} \left[\frac{x_{\text{lin,W}}}{1} \right] \\ x_{\text{dBm}} &= 10 \log_{10} \left[\frac{x_{\text{lin,W}}}{10^{-3}} \right] = x_{\text{dBW}} + 30 \end{aligned} \quad (3)$$

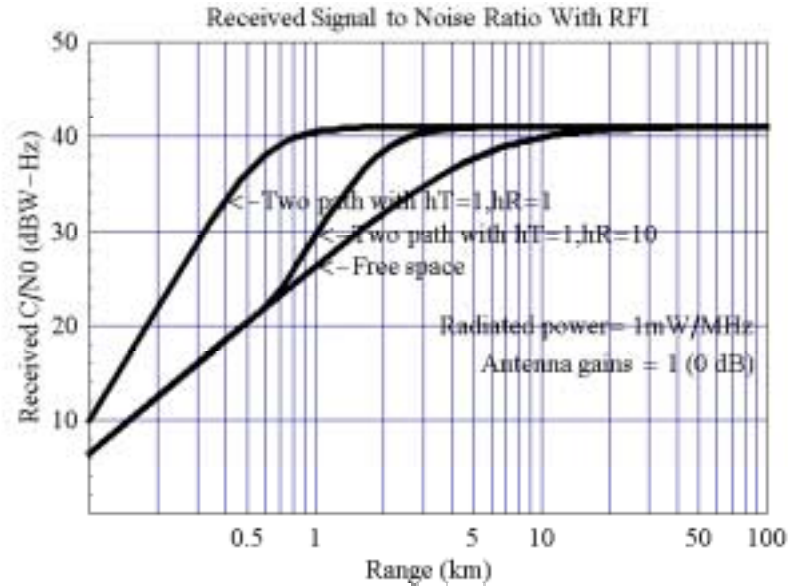
The received signal is amplified by the gain of the user's receiving antenna, G_R , to yield the effective carrier power C . Even in the absence of RFI, the GPS signal must still compete with natural noise received by the antenna and generated in the front end of the receiver. The external noise is given by kT_A , where k is Boltzmann's constant, and T_A is the temperature of the external noise. The receiver's internal noise is given by $kT_0 F_{LNA} L_{\text{cable/filter}}$, where T_0 is a reference temperature of 290 K, F_{LNA} is the noise figure of the low noise amplifier (LNA), and $L_{\text{cable/filter}}$ is the loss of the cable and filter that precede the LNA. This noise density is denoted N_0 , which is a power per unit bandwidth, and typical values are around -201 dBW/Hz.

If man-made signals other than GPS are being received, then we have radio frequency interference (RFI) and the denominator contains an additional term I_0 , which is also a power per unit bandwidth. If an obstruction attenuates the signal, then the numerator of our signal to noise ratio suffers, and the received signal power is reduced by L_{block} . The signal to noise ratio is reduced to

$$\frac{C}{N_0} = \frac{L_{\text{block}} G_R P_S}{N_0 + I_0} = \frac{L_{\text{block}} G_R P_S}{kT_A + kT_0 (F_{LNA} L_{\text{cable/filter}}) + I_0} \quad (4)$$

In general, I_0 depends on the range to the source of the RFI and the details of the propagation path. Figure 1 approximates the signal to noise ratio (C/N_0) assuming that the RFI transmitter is radiating 1 mW/MHz, and that there is no blockage ($L_{\text{block}}=1$). As shown, the signal to noise ratio suffers out to distances of ten kilometers.

Figure 1: Received Signal to Noise Ratio With RFI. A modest radiation of 1 mW/MHz can degrade GPS SNRs to ranges of 1 to 10 kilometers depending on the propagation path from the RFI source to the GPS victim receiver.



Signal obstructions pose a similar challenge. More and more GPS users find themselves in environments that block satellite signals. For example, cell phone users want to be able to automatically communicate their position when they dial 911 to report an emergency. However, they want this capability even if they are downtown or indoors. Under open sky, the C/N_0 for GPS satellites range from 40 to 50 dB-Hz. Downtown, C/N_0 values range from 15 to 40 dB-Hz. Indoors, even the strongest C/N_0 is probably weaker than 25 dB-Hz (Van Roy, et.al.).

These twin challenges, RFI and signal obstructions, have motivated a large family of counter-measures.

Civil aviation operations that use GPS have specified procedures for escaping the area troubled by RFI. Others use inertial guidance to help escape or perhaps complete the operation. Some simply require backup navigation aids such as Loran-C or distance measuring equipment (DME).

Military applications of GPS frequently include beam steering antennas that selectively null out interfering signals without appreciably degrading the signal strength from the GPS satellites. Some of these advanced antennas leverage the direction of arrival of the offending signal and other discriminate based on the polarization of the interfering wave. Such antennas are called *null-steering* or *controlled radiation pattern antennas* (CRPAs). These antennas are a subject of their own, and the interested reader is referred to Compton (1988), Applebaum (1976) and Widrow (1967). Other military receivers incorporate inertial measurements to reduce their

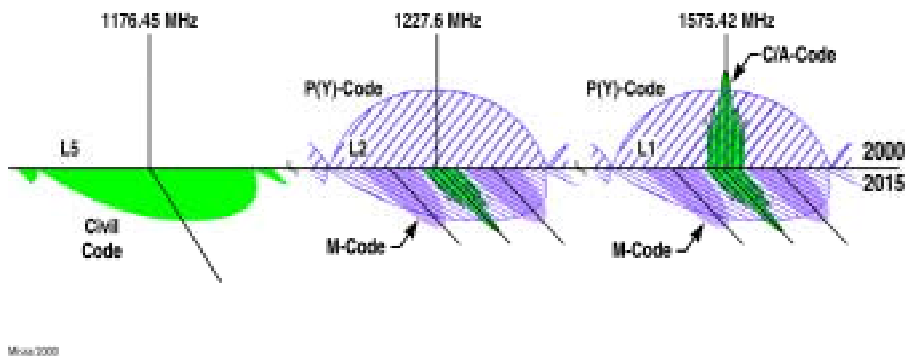
tracking bandwidths and thus reduce the impact of RFI. The Joint Precision Approach and Landing System (JPALS) will use both beam steering and inertial aiding.

Consumer applications may well augment GPS with range measurements to television stations or to cell phone base stations. (Rabinowitz and Spilker, 2003). They also benefit from GPS assistance data that is communicated by the cell phone signals. (Agarwal, et.al. 2002, Enge, Fan and Tiwari, 2001; Taylor and Sennott, 1984; and Syrjarinne, 2001.) The assistance data improves GPS coverage in urban areas by supplanting the fragile navigation message. The replacement navigation message is most welcome, because signal blockages wreak havoc with the navigation messages from the satellites. The cell phone network also delivers estimates of the satellite Doppler, which is used to decrease the signal search area and thereby improves signal sensitivity by enabling the mobile receiver to use longer averaging times. Finally, the cell phone carrier can be used to frequency lock the local oscillator in the mobile receiver, thus improving its stability and further reducing the Doppler search.

4 New Civil Signals

In the near future, GPS will provide an expanded signal set for both military and civil users. Figure 2 shows the signals that are available today along with the new signals. The current signals are described in Section 4.1, and the new signals at $L_2=1227.60$ MHz and $L_5=1176.45$ MHz are described in Sections 4.2 and 4.3 respectively. This paper focuses entirely on the civil signals and capabilities. We spend little time with the old or new military signals.

Figure 2: New & Old GPS Signals: Power Spectrum. In 2000, GPS satellites radiate C/A-coded and Y-coded signals at 1575.42 MHz, and a Y coded signal at 1227.60 MHz. By 2015, they will radiate civil signals at 1575.42, 1227.60 and 1176.45 MHz. They will also radiate new military signals at 1575.42 and 1227.60 MHz.



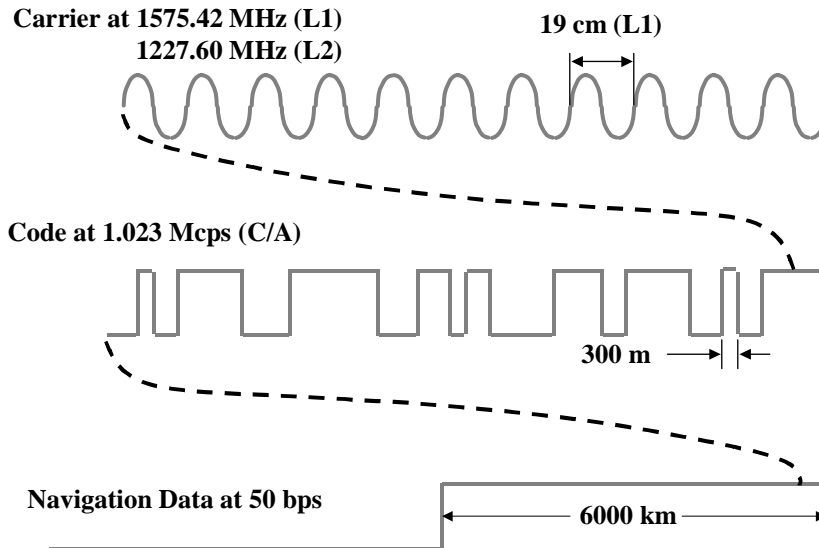
4.1 Today's Civil Signal

The spectra of today's GPS signals are shown in Figure 2. The signal from the k^{th} satellite can be described mathematically as follows:

$$\begin{aligned}
s_{L1}^{(k)}(t) &= \sqrt{2P_C} D^{(k)}(t) x^{(k)}(t) \cos(2\pi f_{L1}t + \theta_{L1}) \\
&\quad + \sqrt{2P_{Y1}} D^{(k)}(t) y^{(k)}(t) \sin(2\pi f_{L1}t + \theta_{L1}) \\
s_{L2}^{(k)}(t) &= \sqrt{2P_{Y2}} D^{(k)}(t) y^{(k)}(t) \sin(2\pi f_{L2}t + \theta_{L2})
\end{aligned} \tag{5}$$

As shown, each satellite sends three rather similar signals. Any of these can be described as the product of four terms: an amplitude $\sqrt{2P}$; the navigation data, $D(t)$; a *spread spectrum code*, $x(t)$ or $y(t)$; and the radio frequency (RF) carrier $\cos(2\pi ft + \theta)$ or $\sin(2\pi ft + \theta)$. This hierarchy is shown in Figure 3.

Figure 3: Hierarchy of GPS Signals Showing Relationship Between the Carrier, Code and Navigation Data. The C/A coded signal on 1575.42 MHz is used as an example.

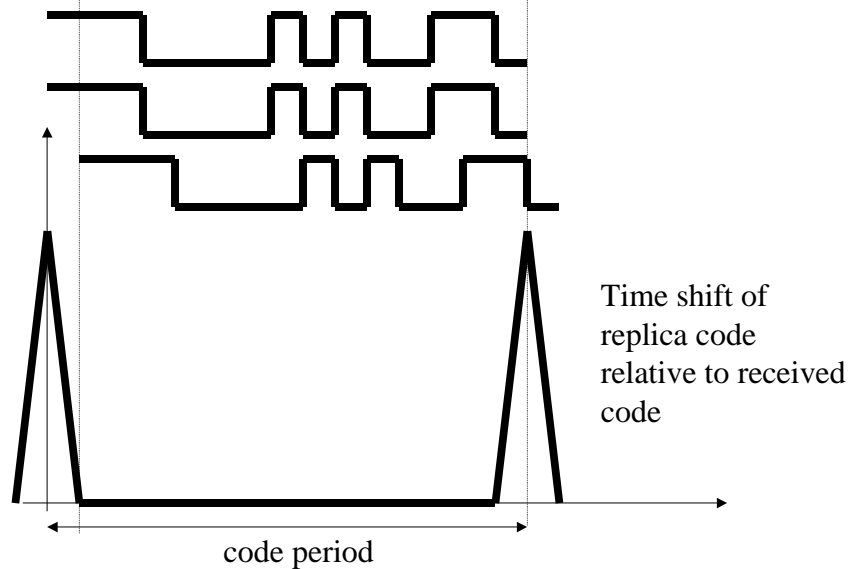


The first signal, with amplitude $\sqrt{2P_C}$, is the basis for the vast majority of civil applications. For compactness, we sometimes refer to it as the civil signal, even though the military also uses this signal. The carrier frequency is $f_{L1}=1575.42$ MHz for all satellites. However, the codes, $\{x^{(k)}(t) | k = 1 \dots K\}$ are unique to each the satellite. These codes are called C/A codes and they spread the spectrum of the transmitted signal. In fact, GPS is a direct-sequence, spread-spectrum system. The C/A codes are sequences of chips each having a polarity of either +1 or -1, and these chips modulate the transmitted signal. The chipping rate for the C/A codes is 1.023×10^6 chips/second, and so the duration of a single chip is approximately 1 microsecond or 300 meters.

The C/A chipping rate also means that the null-to-null bandwidth is 2.046 MHz. This bandwidth is much greater than the bandwidth normally required to send the 50 bps data rate required for the navigation message, $D(t)$. As discussed below, the codes enable precise ranging measurements and allow the receiver to distinguish the signals from the different satellites.

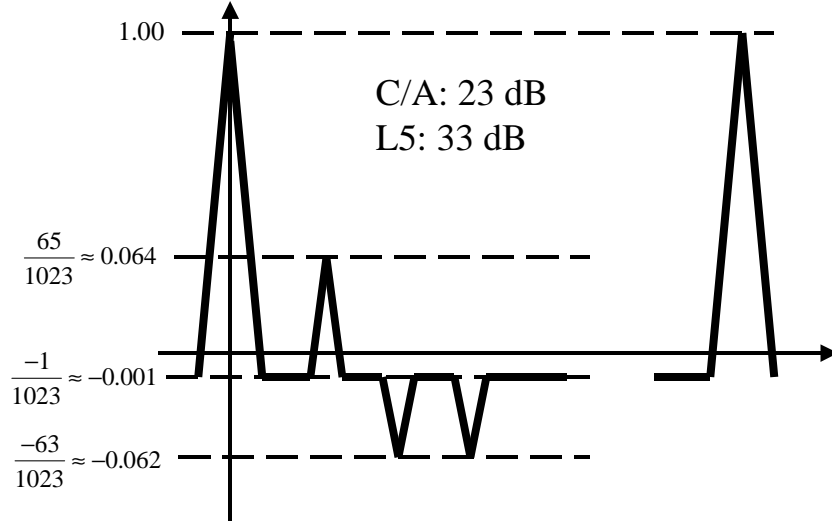
The second and third signals have amplitudes $\sqrt{2P_{Y1}}$ and $\sqrt{2P_{Y2}}$. The military is the main beneficiary of these latter signals, and so we refer to them as the military signals. One of the military signals is broadcast in phase quadrature with the civil signal at $f_{L1}=1575.42$ MHz. In other words, the civil signal modulates $\cos(2\pi f_{L1}t + \theta)$ and the military signal modulates $\sin(2\pi f_{L1}t + \theta)$. The second military signal has a carrier frequency of $f_{L2}=1227.60$ MHz. At present, there is no civil signal at L2. Both military signals are modulated by the so-called Y codes or $y(t)$, and these codes are known only to authorized users. These spectrum spreading codes have chipping rates of 10.23×10^6 chips/second, and so the null-to-null bandwidth is 20.46 MHz. Civil users are permitted to use the Y coded signals, but without the benefit of knowing the Y code. Even without this knowledge, civil users are able to extract some information from L2, but signal tracking is fragile.

Figure 4: Auto-Correlation Properties. The GPS codes are designed to have peaked auto-correlation functions. The main peak is sharp and repeats every code period. It is much higher than any intervening peaks.



The spread-spectrum codes are designed to provide ranging measurements with high precision and without ambiguity. These properties stem from the code's autocorrelation function, which is depicted in Figure 4. As shown, the code is designed so that time-shifted versions of the code will have low correlation with each other. The main peak of the autocorrelation function has steep sides and is much larger than any secondary peaks. The steep sides allow GPS receivers to measure the code phase with high precision. After all, the location of a sharp object is easier to estimate than an object with indistinct or vague edges. The main peak shown in Figure 5 is also significantly larger than any of the secondary peaks, which are also called autocorrelation *sidelobes*. This contrast means that the probability of finding the correct peak is high, and the likelihood of confusing a secondary peak for the main peak is low. Thus the codes provide range measurements with high precision and without ambiguity.

Figure 5: Depiction of Auto-Correlation Function with Sidelobes. The main peak of the C/A code is at least 15.7 times (24 dB) higher than any secondary peak. Even if Doppler effects are included, the main peak is still 23 dB higher than any secondary peaks. The new codes will have even greater discrimination.



The sharpness of the main peak also helps to distinguish the signal arriving directly from the satellite from any signals that have traveled paths that include a reflection. These later signals are called multipath signals and they confound the pseudorange measurements, because they create their own correlation peaks that shadow the main peak created by the direct signal. If the reflected signals are delayed by more than one chip width (300 meters) relative to the direct signal, then the shadow peaks are entirely distinct from the main correlation peak. If distinct, no pseudorange measurement errors result. For shorter delays, the shadow peaks are not distinct from the main peak, and multipath introduces measurement errors.

The GPS codes also have low cross-correlation with each other. More specifically, the cross-correlation is small regardless of the time shift between the codes. With uniformly weak cross-correlation, the signals from the different GPS satellites can usually be distinguished by their codes, and so the satellites broadcast simultaneously without any time sharing or offsets in their transmission frequencies. This nice property is depicted in Figure 6.

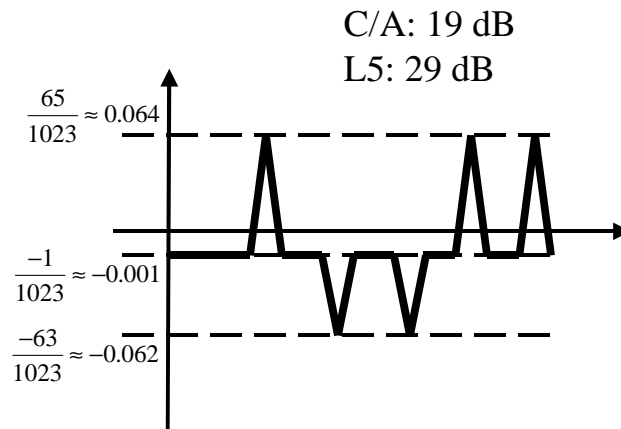
4.2 New Civil Signal at L2

New civil and military signals are planned for $f_{L2}=1227.60$ MHz. The new L2 signal for the k^{th} satellite can be described mathematically as follows:

$$\begin{aligned}
 s_{L_2}^{(k)}(t) = & \sqrt{2P_{Y_2}} D^{(k)}(t) y^{(k)}(t) \sin(2\pi f_{L_2} t + \theta_{L_2}) \\
 & + \sqrt{2P_C} F \{ D_{L_2}^{(k)}(t) \} RC^{(k)}(t) \cos(2\pi f_{L_2} t + \theta_{L_2}) \quad (6) \\
 & + \text{new military M code}
 \end{aligned}$$

The first line in (6) contains the incumbent military signal with Y code modulation, which also appears in (5). The second line contains the new civil signal at L2, and the third line is for the new military signal at L2.

Figure 6: Depiction of Cross-correlation Function With Sidelobes. The main peak of the C/A code is at least 15.7 times (24 dB) higher than any secondary peak. Even if Doppler effects are included, the main peak is still 19 dB higher than any secondary peaks. The new codes will have even better discrimination.



The civil signal is further detailed in Figure 7, which is a functional block diagram of the signal generator. The new code is sometimes called the replacement code (or RC), because it will be used instead of using the C/A code again. The RC does have the same 1.023×10^6 chipping rate as the C/A code and so the null-to-null bandwidth is still 2.046 MHz. However, the RC code is significantly longer. In fact, two codes, CM and CL, are multiplexed to form the RC code. As shown in Figure 7, the CM code has a length of 10,230 chips and so it is 10 times longer than the C/A code. The CL code is even longer with a period of 767,250 chips. This increased length brings some important advantages discussed in Section 5.1.

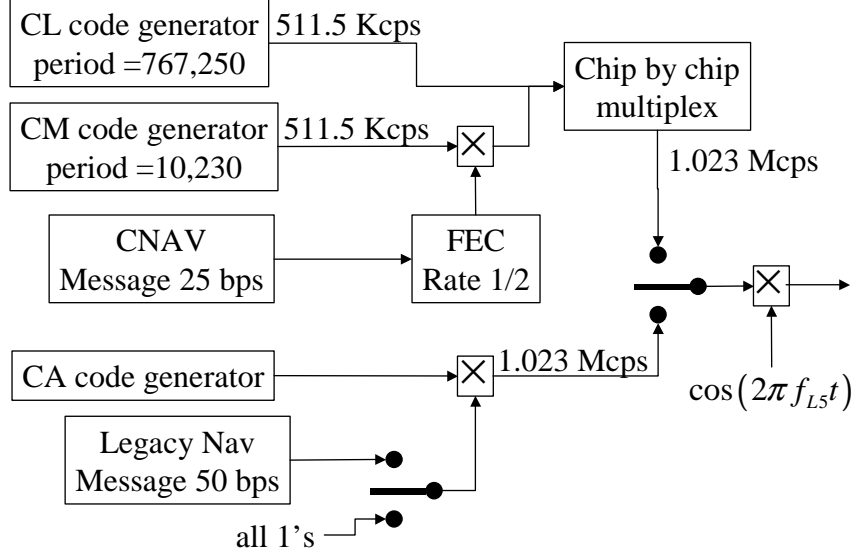
As shown in Figure 7, the two codes alternate, with the CM code controlling every second chip that is broadcast. In this way, the two codes are time multiplexed. The CL code is not modulated by navigation data. This data-free signal is very helpful for operation in low signal to noise ratio environments as we shall discuss in Section 5. The CM code, in contrast, is modulated by navigation data. This data is encoded for forward error correction (FEC) and this feature is also discussed in Section 5.

As shown in Figure 7, the satellite will be able to broadcast the RC code or the C/A code. If the C/A code is broadcast, the satellite will be able to include the navigation data or switch to a data-free C/A code. The switches in Figure 7 allow for these contingencies.

Importantly, the L2 signal does not fall in an Aeronautical Radio Navigation System band (ARNS), and so it does not enjoy the same institutional protection that the L1 and L5 signals do.

Figure 7: New Civil Signal at L2: 1227.60: A Functional Block Diagram

$$s_{L2}^{(k)}(t) = \sqrt{2P_C} F \left\{ D_{L2}^{(k)}(t) \right\} RC^{(k)}(t) \cos(2\pi f_{L2}t + \theta_{L2})$$



4.3 New Civil Signal at L5

A new civil signal is planned for $f_{L5}=1176.45$ MHz. The new L5 signal for the k^{th} satellite can be described mathematically as follows:

$$s_{L5}^{(k)}(t) = \sqrt{2P_G} F \left\{ D^{(k)}(t) \right\} NH_{10}(t) g_1^{(k)}(t) \cos(2\pi f_{L5}t + \theta_{L5}) + \sqrt{2P_G} NH_{20}(t) g_2^{(k)}(t) \sin(2\pi f_{L5}t + \theta_{L5}) \quad (7)$$

No military signal is planned for L5, and so the inphase ($\cos(2\pi f_{L5}t + \theta_{L5})$) and quadrature ($\sin(2\pi f_{L5}t + \theta_{L5})$) components are both used for civil signals.

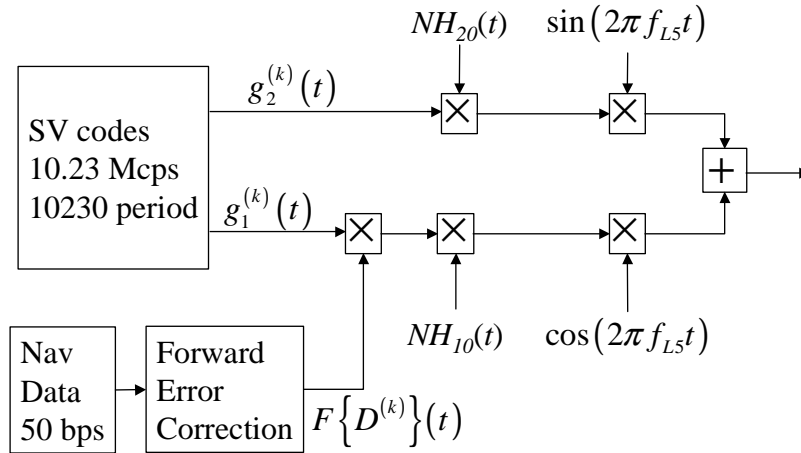
The L5 civil signal is further detailed in Figure 8, which is a functional block diagram of the signal generator. As shown, the inphase signal from the k^{th} satellite is modulated with the $g_1^{(k)}(t)$ code and navigation data. The navigation data requires 50 bps, but forward error correction is applied and so the final symbol rate is 100 symbols per second (sps).

The quadrature component is modulated with the $g_2^{(k)}(t)$ code, but no navigation data is applied. Like the new L2 signal, the new L5 signal also provides a data free signal component to enhance operation at low signal to noise ratios. However, the L5 signal design did not have to resort to time multiplexing of the codes, because both the inphase and quadrature channels were available for civilian use.

Both codes, $g_1^{(k)}(t)$ and $g_2^{(k)}(t)$, are 10,230 chips long. Both are sent at rates of 10.23 Mcps, and so the null-to-null bandwidth is 20.46 MHz. This increase in bandwidth brings benefits that are described in Section 5.

Figure 8: New GPS Signal at L5: 1176.45 MHz: A Functional Block Diagram

$$s_{L5}^{(k)}(t) = \sqrt{2P_G} F\{D^{(k)}\}(t) NH_{10}(t) g_1^{(k)}(t) \cos(2\pi f_{L5}t + \theta_{L5}) + \sqrt{2P_G} NH_{20}(t) g_2^{(k)}(t) \sin(2\pi f_{L5}t + \theta_{L5})$$



As shown in Figure 8, Neumann-Hoff codes also modulate the inphase and quadrature channels. These codes are short and simply serve to extend the length of the $g_1^{(k)}(t)$ code from 10,230 chips to 102,300 chips, and extend the length of the $g_2^{(k)}(t)$ from 10,230 chips to 204,600 chips. With a chipping rate of 10.23 Mcps, the $NH_{10}(t)g_1^{(k)}(t)$ code period is 10 ms long, and is equal to the duration of a FEC-encoded navigation bit (10 ms at 100 sps). The $NH_{20}(t)g_2^{(k)}(t)$ has a period of 20 ms.

Like the L1 signal and unlike the L2 signal, the new L5 signal resides in an ARNS band. Hence, L1 and L5 processing will be preferred by avionics designed to serve safety critical applications. However, the new L5 band does fall in the middle of the band currently used by distance measuring equipment (DME) worldwide and used for the Joint Tactical Information Distribution System (JTIDS) in the United States. As a result, the L5 noise floor will frequently be higher than thermal noise (N_0) especially for aircraft at significant altitudes. Fortunately, the radiated power will be approximately four times greater than the current C/A signal power, and the U.S. FAA is prepared to reallocate DME frequencies in the U.S. if needed.

5 Improved Signal Acquisition and Tracking Using L2 and L5

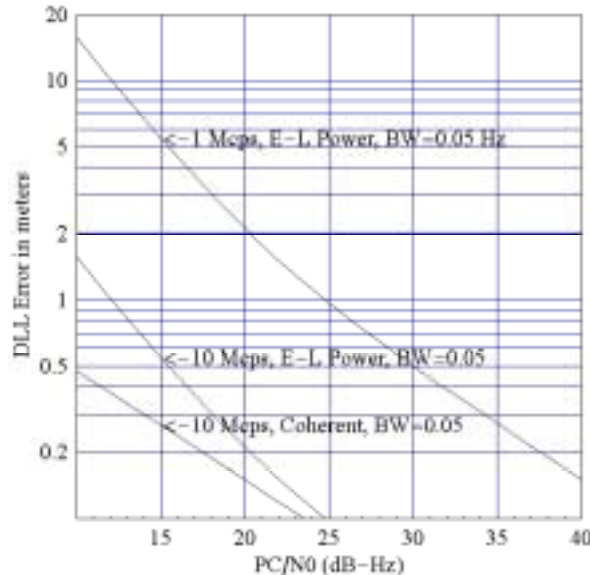
The new GPS signals bring immediate improvements to signal acquisition and tracking. The following properties are beneficial: faster codes, longer codes, forward error correction, and data-free signal components. We now describe these features in turn.

5.1 Faster codes on L5

The code on L5 will be ten times faster than today's C/A code. The chipping rate will be 10.23 Mcps instead of 1.023 Mcps. This increase in speed brings a number of advantages. First,

the higher chipping rate on L5 will make the main peak in the auto-correlation function sharper by a factor of ten. By so doing, the new signals improve the noise performance of the GPS receivers, and this improvement is shown in Figure 9. The sharper peak also makes it easier for the receiver to resolve and mitigate the effects of multipath, and this improvement is depicted in Figure 10.

Figure 9: Benefits of Faster Codes to Tracking. The existing L1 codes have chipping rate of approximately 1 Mcps, while the new L5 codes will have chipping rates of 10 Mcps. The increased speed reduces the tracking error.



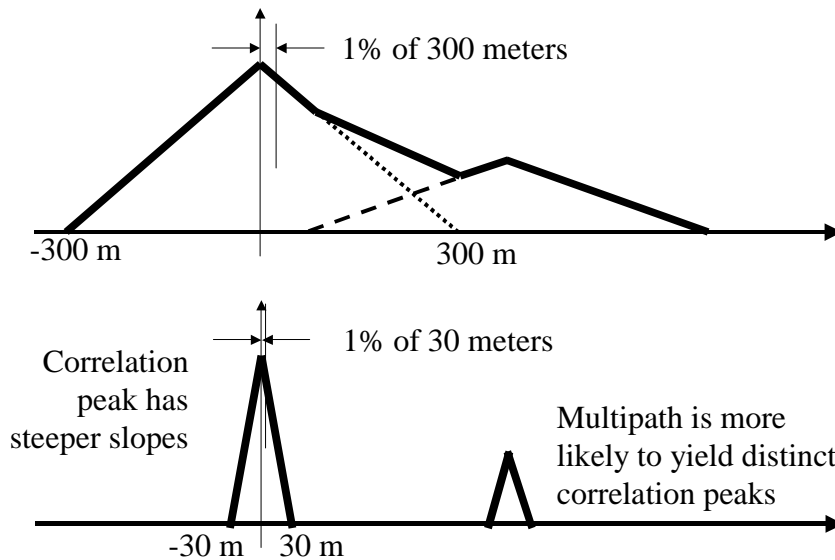
Finally, the ten-fold increase in bandwidth increases resistance to broadband RFI. Taken together with the four times increase in power, the L5 signal will be significantly less vulnerable to RFI.

5.2 Longer codes on L2 and L5

The increased length of the codes at L2 and L5 means that the auto-correlation and cross-correlation sidelobes are lower than that for the C/A code. Specifically, the worst sidelobe for the C/A code is approximately 23 dB weaker than the main lobe. In contrast, the worst sidelobe for the new L5 codes is approximately 33 dB weaker than the main lobe. Similarly, the worst sidelobe for the cross-correlation function drops from approximately -19 dB to -29 dB for the new L5 codes. These improvements are depicted in Figures 5 and 6. Both improvements reduce the probability of false lock during signal acquisition. The reduction in cross-correlation interference is particularly helpful when the desired signal is obstructed and therefore much weaker than signals from other satellites.

The longer codes also decrease the spacing between the lines in the GPS signal spectrum by a factor of ten. With ten times the number of lines, the amount of energy per line is diminished by the same factor of ten. This reduces the worst case effect of narrowband RFI by 10 dB. (Spilker and Van Dierendonck, 2001 and RTCA DO-235).

Figure 10: Faster Codes Improve Multipath Performance. The L1 codes can resolve reflections that are delayed by 300 meters or more. In contrast, the L5 codes will be able to resolve multipath delayed by 30 meters or more.



5.3 Forward error correction (FEC)

As mentioned in Section 4.2 and 4.3, forward error correction (FEC) is used with the new signals. It is used to correct bit decision errors suffered while demodulating the navigation message. The improvement is shown in Figure 11, which compares the probability of bit error performance for the encoded signal to the present signal. As shown, FEC bring a 5 dB improvement in performance.

5.4 Data-free signal components

As described in Sections 4.2 and 4.3, both new signals have data-free components. Since the new L2 signal must co-exist with the existing military signal, it time multiplexes the CM and CL codes. The CL code is not modulated with data, and the CM code is modulated with data. The new L5 signal will not co-exist with a military signal, and so the data-free signal is in phase quadrature with the signal that has data modulation.

Data-free signal components are very useful in low signal-to-noise (SNR) ratio environments. Since the navigation bits are not known a-priori, today's GPS receiver must square the received signal to strip the navigation bits. This squaring action achieves the intended purpose of removing the data modulation, but it also introduces squaring loss. Squaring loss arises simply because the received noise is also squared. It grows as the SNR decreases. Unfortunately, squaring loss is greatest in low SNR environments.

Today, some GPS receivers that are designed for low SNR environments strive to predict future navigation bits based on the recent history of navigation bits. This technique usually works rather well, because the navigation bits do not change rapidly. However, the satellite updates its navigation message every two hours or so. At this time, prediction is impossible.

Figure 11: Pr(Bit Error) With & Without FEC. The new L2 and L5 signals employ forward error correction to recover lost bits in the navigation message. This yields a 5 dB improvement in signal to noise ratio performance.

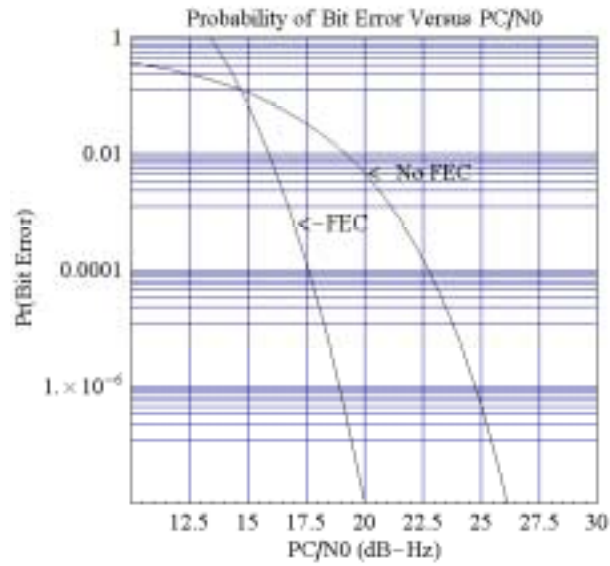
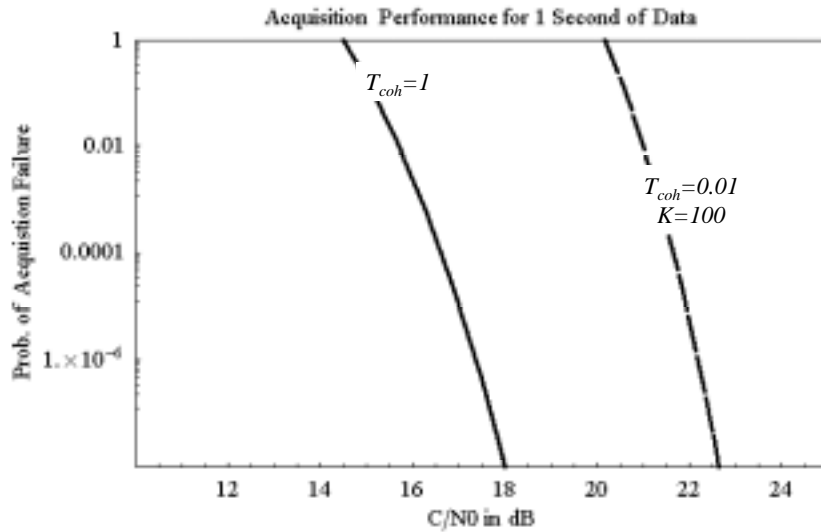


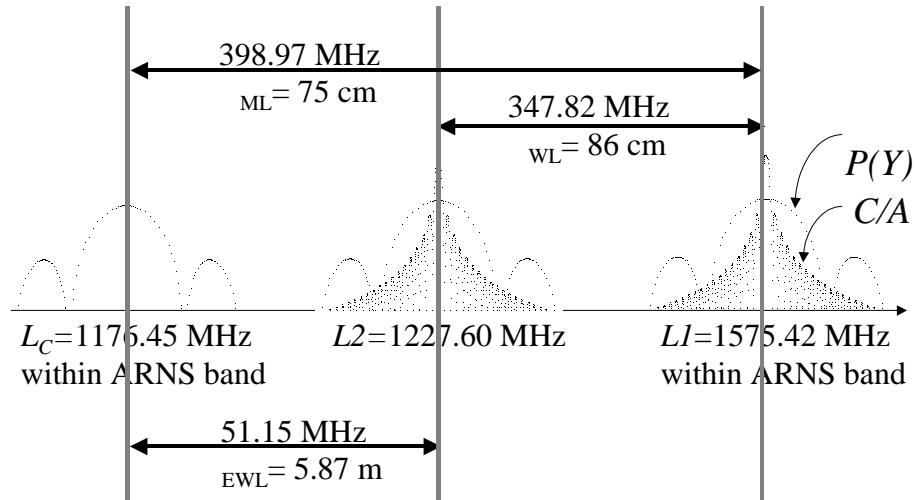
Figure 12: Benefits of Data-Free Signal on the Probability of Failed Acquisition: The new L2 and L5 signals have data-free channels that will provide the indicated improvements in the signal to noise ratio required to acquire a signal.



The new signals will obviate this struggle by including data-free signal components. This relief can be seen in Figure 12, which shows the probability that a receiver will incorrectly identify the time of signal arrival when trying to acquire new signals. The curve marked $T_{coh}=1$ s averages the incoming measurements for one second and does not square the signal. The curve marked $T_{coh}=0.01, K=100$ also averages for a total of one second, but squares the data every 0.01

seconds. The data free signal enables the former approach, and as shown affords a 4 dB improvement in performance.

Figure 13: Ionospheric Measurement: The ionospheric delay is dispersive, and so measurements at multiple frequencies can be used to estimate this delay. As shown, the two new civil signals provide multiple opportunities to make such a measurement.



6 Frequency Diversity for Ionospheric Estimation

Three civil frequencies will allow users to remove the ionospheric delay, which is the largest GPS error source. More specifically, the new signals will enable the following performance hierarchy:

- Legacy users will continue to operate as before. Some will derive an ionospheric estimate from the single frequency ionospheric model included in the GPS navigation message. Others will use differential GPS to remove most of the ionospheric error, but with the cost of a reference receiver and data link. Single frequency users of SBAS will continue to use the real time ionospheric model contained in that data stream.
- Aviation users will use the two ARNS frequencies, L1 and L5, to estimate the ionospheric delay in the aircraft. They will enjoy a significant increase in SBAS coverage as discussed in Section 6.1 below. They will also find that receiver autonomous integrity monitoring (RAIM) is more effective. Avionics will revert to single frequency use in the presence of RFI.
- Non-aviation users will be able to estimate the ionosphere from any pair of frequencies. The traditional L1/L2 combination and the new L1/L5 combination will be the best, because the frequency differences are 348 and 399 MHz respectively. The L2/L5 combination will be less effective for ionospheric estimation, because the frequency difference is only 51 MHz. These frequency differences are shown in Figure 13.
- High precision (centimeter and decimeter) users will be able to use all three frequencies to great advantage. If they desire centimeter accuracy, they will still require differential

reference receivers, but the rovers will be able to travel to much farther from these information anchors. They will be able to achieve decimeter accuracy without differential operation. These improvements are discussed in Section 6.2.

6.1 Two ARNS Frequencies Enable Airborne Estimation of Ionospheric Delay

The new ARNS signals, at L5, will significantly increase the utility of WAAS and LAAS. They will enable the avionics to estimate the ionospheric delay autonomously. At present, both LAAS and WAAS are limited by the *prospect of an ionospheric gradient*. In other words, the protection levels are conservative, because they must account for the possibility that the ionospheric delay at the reference station may differ from the ionospheric delay at the aircraft.

For example, today's, single frequency, WAAS provides the coverage shown in Figure 14 (Jan, 2003). The darkest area shows where the vertical protection level (VPL) is less than 50 meters and the horizontal protection level (HPL) is less than 40 meters more than 99.9% of the time. The 50 and 40 meter values are significant, because they enable vertical guidance for most of the airports in the United States. As shown, today's coverage roughly corresponds to the boundary of the conterminous United States. Such a boundary makes sense, because it corresponds to the area where the ionosphere is densely sampled. Absent a dense ground network, the protection levels will grow to accommodate the prospect of an ionospheric gradient. In other words, the protection levels are low only where the reference receivers are dense.

In contrast, Figure 15 predicts WAAS coverage for future aircraft that would carry dual frequency WAAS receivers (Jan, 2003). This equipment would apply the fast and long term corrections from WAAS to correct for satellite-specific errors. Then, it would measure the ionospheric delay locally in the avionics. Hence, it could ignore the ionospheric grid broadcast by WAAS and employ more aggressive protection levels. As shown, the coverage area grows significantly.

The L5 signal will have an equally important effect on LAAS. Single frequency LAAS will be able to provide vertical guidance down to altitudes of 200 feet or so. In the parlance of aviation, single frequency LAAS will support Category I precision approach. A single frequency LAAS architecture may also support Category II approaches, where guidance will be provided to 100 decision heights, and it may support Category III approaches that include landings in zero visibility conditions. However, all of these LAAS operations will have reduced availability due to the prospect of ionospheric gradients. They will also require backup landing systems to cope with the prospect of RFI. After L5 is available, LAAS combined with inertial aiding should be able to support all approach operations including blind landings with high availability.

6.2 Three Frequencies Enable Geometry-Free Integer Determination

Many non-aviation applications require centimeter or decimeter accuracies. These high-end applications measure the phase of the GPS carrier signal at the roving receiver relative to the phase at a nearby reference receiver. This GPS-based phase interferometer constitutes the high end of the GPS accuracy capability, and is called differential carrier phase GPS in the aviation community and real time kinematic (RTK) in the survey community.

If the user is within 10 kilometers of the reference receiver, then centimeter accuracy can be achieved. If the user is within 100 kilometers, then decimeter accuracy can be achieved. These accuracy levels can be achieved in real time provided the reference station is connected to the roving receiver with a data link that can carry 1000 bps or more. Current research strives to

increase the distance between the rover and the reference and to reduce the bandwidth required for the data link.

Figure 14: WAAS Availability with Single Frequency Avionics. The contours show the fraction of time that the WAAS can protect vertical errors of 50 meters and horizontal errors of 40 meters. Coverage is limited to areas where the reference station network is dense (Jan, 2003).

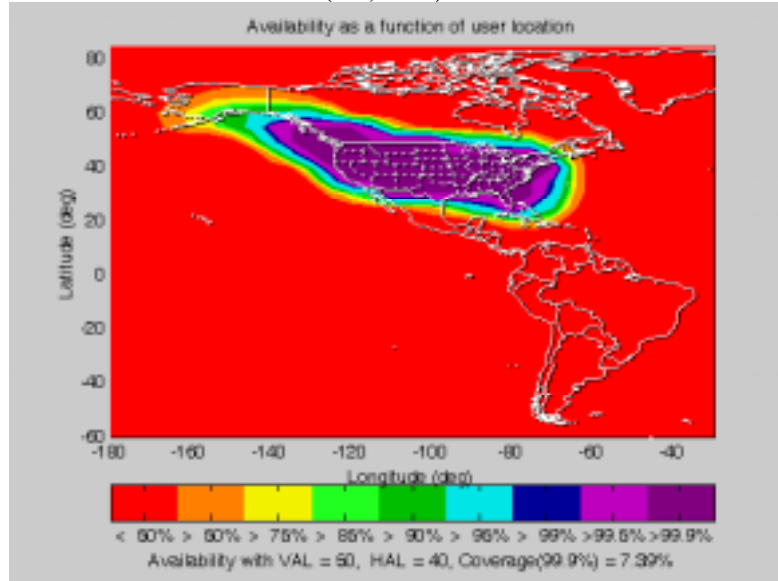
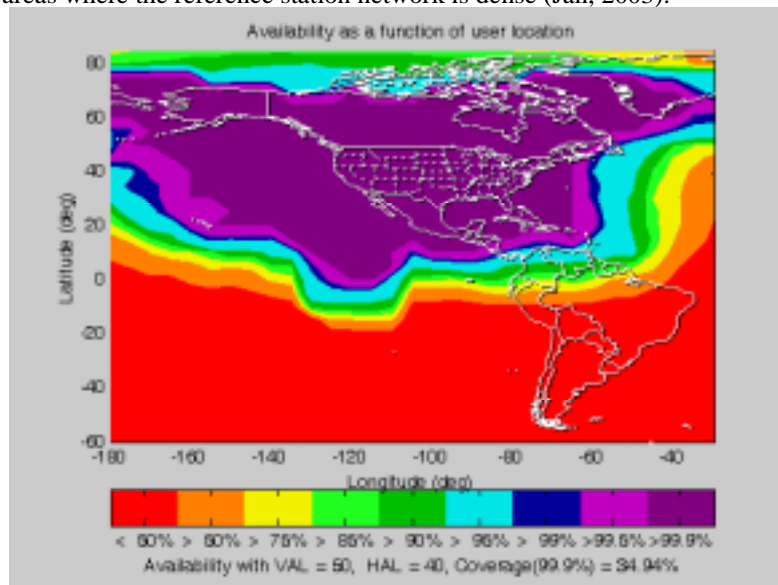


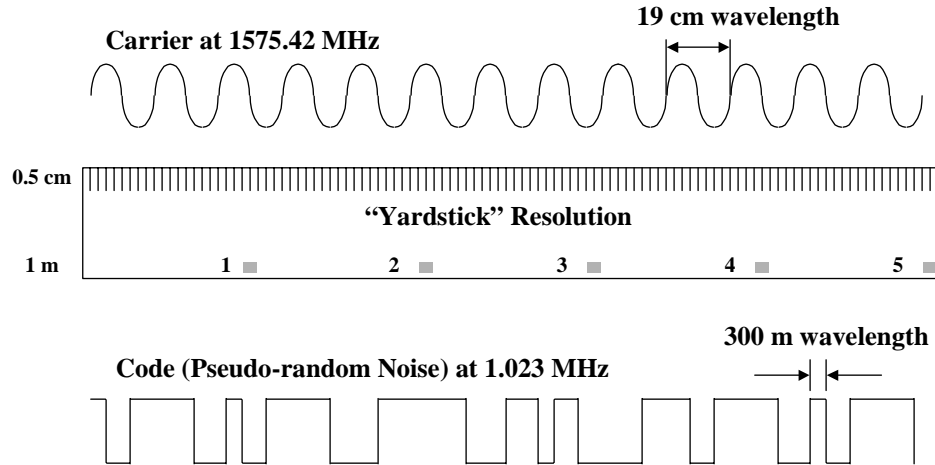
Figure 15: WAAS Availability with L1-L5 Avionics. The contours show the fraction of time that the WAAS will be able to protect vertical errors of 50 meters and horizontal errors of 40 meters. The 99.9% contours have spread well beyond the areas where the reference station network is dense (Jan, 2003).



RTK leverages the precision of the carrier phase. Relative to code phase measurements, carrier phase measurements gain precision at the expense of ambiguity. Code phase

measurements are akin to the coarse, but unambiguous marks on the bottom of the yard stick depicted in Figure 16. Each of these is associated with a number, and so they are unambiguous. Carrier phase measurements are akin to the fine but ambiguous marks on the top of the ruler. They provide precision, but we do not easily know how many fine marks are included in our measurement, because the fine ticks are not individually marked with a number.

Figure 16: GPS Code and Carrier Measurements. Code phase measurements are akin to the coarse, but unambiguous marks on a yard stick. Carrier phase measurements are akin to the fine but ambiguous marks in between the code phase measurements. The figure is not to scale.



A single wavelength of the GPS carrier at L1 is approximately 19 cm long, and is akin to the fine marks on the ruler. The receiver can measure carrier phase to a fraction of this wavelength. Unfortunately, the receiver can only measure the fractional wavelength difference between the reference and rover phases, but cannot directly measure the number of whole cycles contained in the phase difference. In other words, the measured phase difference is modulo 2 and the receiver must employ special RTK algorithms to determine the N term that is also contained in the measurement. This integer problem has been the subject of many scholarly works, and quite a few commercial products.

If L1 is the only available frequency, then integer resolution requires tens of minutes. Essentially, the rover must wait for the satellites to move appreciably across the sky and render the integers observable. If L1 and L2 are both available, then *wide-lanes* are formed, and integer resolution can be achieved in tens of seconds. The L1 and L2 signals are multiplied to form the wide lanes as follows:

$$\begin{aligned}
 & \sqrt{2P_{Y1}} D^{(k)}(t) y^{(k)}(t) \sin(2\pi f_{L1}t + \theta_{L1}) \times \sqrt{2P_{Y2}} D^{(k)}(t) y^{(k)}(t) \sin(2\pi f_{L2}t + \theta_{L2}) \\
 & = \sqrt{P_{Y1}P_{Y2}} \left[\cos(2\pi(f_{L1} - f_{L2})t + \theta_{L1} - \theta_{L1}) - \cos(2\pi(f_{L1} + f_{L2})t + \theta_{L1} + \theta_{L1}) \right]
 \end{aligned} \tag{8}$$

The difference term is called the wide lane, because it has a wavelength of $\lambda_{\text{WL}} = c/(f_{L1} - f_{L2}) = 86$ cm, where c is the speed of light. The sum term is called the narrow lane, because $\lambda_{\text{NL}} = c/(f_{L1} + f_{L2}) \approx 10.7$ cm. The wide lane serves as a stepping stone from the code phase measurements to the carrier phase measurements. If the unambiguous code phase measurements are averaged, then they may have enough precision to identify the number of whole wide lanes in the rover to reference phase difference. After the wide lane ambiguity is resolved, further averaging is used to resolve the 19 cm L1 ambiguity.

Wide lanes are helpful, but the step from code phase measurements to wide lane integers is still ambitious. After all, a geometry-free integer determination would require the code phase error to be smaller than 86 cm. Such performance is stretching the capability of code phase measurements unless the rover is quite close to a DGPS reference receiver.

Even if the integer ambiguity is correctly resolved, the wide lane does not offer a low noise measurement of the range to the satellite. Rather, it offers a low noise measurement of the range plus the ionospheric delay. The measured widelane for the k^{th} satellite is

$$\lambda_{\text{WL}}\phi_{\text{WL}}^{(k)} = r^{(k)} + 1.28I_{L1}^{(k)} \quad \text{m} \quad (9)$$

In this equation, $\lambda_{\text{WL}}\phi_{\text{WL}}^{(k)}$ is the measured widelane after the integer ambiguity has been removed. The true range is contained in $r^{(k)}$, which also includes the clock offsets, measurement noise and all non-dispersive effects such as the tropospheric delay. The ionospheric delay is given by $I_{L1}^{(k)}$, and the subscript acknowledges the frequency dependence of this delay. As shown, the desired estimanda appear in combination with the ionospheric nuisance parameter.

Fortunately, the third civil signal addresses both of the above-described problems. First, the wavelength formed by the L1 to L5 beat frequency of 400 MHz is 65 cm, and so it is called the medium lane. The wavelength formed by the L2 to L5 difference of 50 MHz is 2 meters, and so it is called the extra wide lane (EWL). Both of these new frequencies have integer ambiguities also, but the EWL is more readily resolved by a code phase measurement (Jung, 1999). Once resolved, the EWL measurement provides a stepping stone to the wide lane of 86 cm.

Moreover, the new measurements also enable the separation of the non-dispersive delays from the ionospheric delay. The measurements at the two new beat frequencies are

$$\begin{aligned} \lambda_{\text{EWL}}\phi_{\text{EWL}}^{(k)} &= r^{(k)} + 1.72I_{L1}^{(k)} \quad \text{m} \\ \lambda_{\text{ML}}\phi_{\text{ML}}^{(k)} &= r^{(k)} + 1.34I_{L1}^{(k)} \quad \text{m} \end{aligned} \quad (10)$$

As shown in these equations, the wide lane, extra wide lane, and medium lane have different dependencies on the ionospheric delay, and so the ionospheric delay can be separated from the non-dispersive delay contained in all of the measurements.

7 Summary

GPS modernization includes three mega-trends: integrity machines, RFI hardening and signal diversity. The first integrity machine is the U.S. Wide Area Augmentation System or WAAS, which began aviation use on July 10, 2003. The European equivalent is scheduled to begin operation in 2004, and the Japanese version will not be far behind. India and China are

also developing space-based augmentation systems. Local area augmentation systems are also being developed worldwide, and precision approach operations will begin in a few years. In addition, Australia has pioneered a ground based regional augmentation system (GRAS). All of these machines are important – they protect the users by adding a bound on the inaccuracy of the system.

All satellite navigation systems must be hardened to withstand the effects of radio frequency interference (RFI). After all, the signals travel some 20,000 kilometers from orbit to the users they serve. Protection will be gained either from hardening the basic GPS engine with beam steering antennas or incorporating redundant sensors. Some applications will incorporate the new sensors directly into the GPS receiver, and some will simply run a redundant positioning engine in parallel.

Finally, GPS modernization includes frequency diversity for the satellite signals. Within the decade, GPS satellites will broadcast civil signals at three frequencies: L1, L2 and L5. The new signals will use longer codes, and in the case of L5, faster chipping rates. Both of the new frequencies will also carry data-free signal components. These measures will significantly improve the signal acquisition and tracking performance of the basic GPS engine. The multiplicity of signals will also allow a new level of accuracy and robustness by offering new techniques to remove the ionospheric delay from the measurements. Thus the largest current error source will be eliminated.

All told, GPS will offer some amazing new capabilities in the next decade.

Acknowledgements

The author gratefully acknowledges the support of the Federal Aviation Administration under Grants 95-G-005, 97-G-012 and 00-G-028. He also gives his heartfelt thanks to the large number of colleagues at Stanford University and in the larger aviation navigation community. This paper draws on the work of this dedicated community. However, this paper also includes the personal opinions of the author, and does not necessarily convey the opinions of any other person or organization.

References

1. N. Agarwal, J. Basch, P. Bechmann, P. Bharti, S. Casadei, A. Chou, P. Enge, W. Fong, N. Hathi, W. Mann, A. Sahai, J. Stone, J. Tsitsiklis and B. Van Roy, "Urban GPS: Algorithms for GPS Operation Indoors and Downtown," to be published in GPS Solutions, 2002
2. A. Applebaum, "Adaptive Arrays," IEEE Transactions on Antennas and Propagation, vol. AP-24, no. 5, pp. 585-598, 1976
3. F. Bauregger, "Novel Anti-Jam Antennas for Airborne GPS Navigation," PhD dissertation, Stanford University Department of Aeronautics and Astronautics, 2003
4. J. Blanch, "An Ionosphere Estimation Algorithm for WAAS Based on Kriiging," Proceedings of ION GPS 2002, Portland Oregon, September 24-27, 2002
5. R. Compton, *Adaptive Antennas*, Prentice Hall, 1988
6. P. Daly and P. Misra, "GPS and Global Navigation Satellite System (GLONASS)," Chapter 9 in Volume II of B. Parkinson and J. Spilker, editors, "Global Positioning System: Theory and Applications," American Institute of Aeronautics and Astronautics, 1996

7. P. Enge, R. Fan and A. Tiwari, "GPS Reference Network's New Role: Providing Continuity and Coverage," *GPS World*, Vol. 12, No. 7, July, 2001
8. *Galileo's World*, a magazine published quarterly by Advanstar Communications
9. Shau-Shiun Jan, "Aircraft Landing Using a Modernized Global Positioning System and the Wide Area Augmentation System," PhD thesis, Stanford University Department of Aeronautics and Astronautics, SUDAAR 768
10. J. Jung, "High Integrity Carrier Phase Navigation Using Multiple Civil GPS Signals," PhD thesis, Stanford University Department of Aeronautics and Astronautics, SUDAAR 725
11. P. Misra and P. Enge, "Global Positioning System: Signals, Measurements and Performance," Gunga-Jumuna Press, 2001, available from NavTech Seminars
12. B. Parkinson and J. Spilker, editors, "Global Positioning System: Theory and Applications," American Institute of Aeronautics and Astronautics, 1996
13. S. Pullen, T. Walter and P. Enge, "System Overview, Recent Developments and Future Outlook for WAAS and LAAS," Tokyo University of Mercantile Marine GPS Symposium, Tokyo, Japan, 12 November, 2002
14. M. Rabinowitz and J. Spilker, "The Rosum TV Position Technology," Proceedings of the 59th Annual Meeting of the Institute of Navigation, Albuquerque, June 23-25, 2003
15. RTCA, "Assessment of Radio Frequency Interference Relevant to the GNSS," Report RTCA DO-235, December 5, 2002
16. R. Taylor and J. Sennott, "Navigation System and Method," U.S. Patent No. 4,445,118, April 24, 1984
17. A.J. Van Dierendonck and J. Spilker, "GPS Modernization," *Journal of the Institute of Navigation*, 2001
18. T. Walter, P. Enge and A. Hansen, "Integrity Equation for the WAAS MOPS," Selected Papers on Satellite-Based Augmentation Systems, Published and Invited Paper, Institute of Navigation, 1999
19. B. Widrow, et.al., "Adaptive Antenna Systems," Proceedings of the IEEE, vol. 55, no. 12 pp. 2143-2159, 1967